Int. J. Therm. Sci. (2001) 40, 273–278

S1290-0729(00)01217-5/FLA

Mixing and magnetic effects on a nonequilibrium argon plasma jet

Takehiko Sato [a]*, Masaya Shigeta [b], Daigo Kato [c], Hideya Nishiyama [a]

[a] *Institute of Fluid Science, Tohoku University, 2-1-1 Katahira, Aoba-ku, Sendai, 981-8577, Japan*

[b] *Graduate School of Engineering, Tohoku University, 2-1-1 Katahira, Aoba-ku, Sendai, 980-8577, Japan*

[c] *Nippon Steel Corporation, 20-1 Shintomi, Futtsu, Chiba, 293, Japan*

(Received 30 November 1999, accepted 16 June 2000)

Abstract — Effects of gas admixture and of an applied magnetic field on a nonequilibrium Ar plasma jet are investigated experimentally. The maximum gas temperature and gas velocity are observed in the core region of an Ar/He plasma due to the small density, the large thermal conductivity and Mach number effect of He. Furthermore, their radial gradients become very steep in the applied magnetic field. In contrast, the gas temperature and gas velocity of an Ar/N_2 plasma jet are not so high and their radial gradients are moderate, because of the energy loss needed to dissociate N_2 gas in the core region and of the active thermal diffusion in the radial direction. Electron number density is larger in the case of an Ar/Ar plasma jet or an Ar/He plasma jet compared with that of an Ar/N_2 plasma, since N_2 gas dissociates before ionization. It is shown that the admixing of He or N_2 gas influences controllably the flow and temperature fields of a nonequilibrium Ar plasma jet also in an applied magnetic field. © 2001 Éditions scientifiques et médicales Elsevier SAS

plasma jet / magnetic field / admixing / thermofluid characteristics / plasma properties / thermal nonequilibrium

Nomenclature

B	magnetic flux density	T
$\overline{C}_e$	average thermal velocity of electrons	$m{\cdot}s^{-1}$
C_p	specific heat at constant pressure	$J{\cdot}kg^{-1}{\cdot}K^{-1}$
e	electron charge	C
I_{is}	ion saturation current	A
I_p	probe current	A
k	Boltzmann constant	$J{\cdot}K^{-1}$
l_e	mean free path of electron	m
m_i	mass of ion	kg
m_e	mass of electron	kg
n_e	electron number density	m^{-3}
p_t	total pressure	Pa
p_s	static pressure	Pa
r	radial coordinate	mm
S_p	surface area of Langmuir probe	m^2
T_e	electron temperature	K
T_g	gas temperature	K
T_t	total temperature	K
V_p	probe voltage	V
U_g	gas velocity	$m{\cdot}s^{-1}$
z	axial coordinate	m

Greek symbols

κ	constant	
λ_e	electron thermal conductivity	$W{\cdot}m^{-1}{\cdot}K^{-1}$
γ	specific heat ratio	
μ_e	electron mobility	
$\bar{\nu}_{eH}$	mean collison frequency between electron and heavy particle	s^{-1}
σ_e	electrical conductivity	$S{\cdot}m^{-1}$

1. INTRODUCTION

Plasma is used as a multifunctional medium, because it has high energy density, chemical reactivity and variable transport properties. Therefore, plasma has been utilized for material processing such as cutting, welding and

* Correspondence and reprints.
E-mail addresses: sato@ifs.tohoku.ac.jp (T. Sato), shigeta@paris.ifs.tohoku.ac.jp (M. Shigeta), dkato@par.odn.ne.jp (D. Kato), nishiyama@ifs.tohoku.ac.jp (H. Nishiyama).

spraying, for pollutant waste treatment such as decomposition of dioxin and freon and for melting incombustible waste for reducing its volume. However, only a few fundamental papers have been published about effects of entrainment [1] and the admixing of gases [2, 3] on a DC plasma jet and the effect of an applied magnetic field on it [4, 5]. As well, the admixing effects on an RF inductively coupled plasma has been also clarified in a few papers [6–8]. These papers have shown that the thermofluid characteristics are considerably changed by the admixing of the various kinds of gases under the plasma conditions.

The main objective of the present paper is to clarify experimentally the admixing effects of He and N_2 gases on the thermofluid characteristics and plasma properties of a nonequilibrium Ar plasma jet with and without applying a magnetic field.

2. EXPERIMENTAL SET-UP AND PROCEDURES

Figure 1 shows the experimental apparatus. It consists mainly of a d.c. plasma torch, a test pipe, solenoidal coils and a vacuum system.

Figure 2 shows a plasma torch in detail. It is constructed of a cathode, the primary anode nozzle, the secondary anode nozzle and the third nozzle. The primary gas is Ar of 30 Sl·min^{-1}, which is introduced into the torch with weak swirl flow through the cathode. The discharge power in the primary anode nozzle is 0.9 kW. The secondary gas is Ar, He or N_2, 30 Sl·min^{-1}, which is injected tangentially between the primary anode nozzle and the secondary anode nozzle. Each discharge power

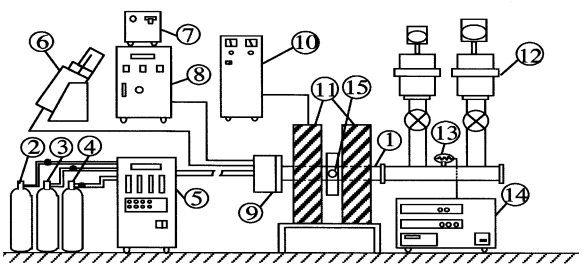

① Test pipe, ② Nitrogen gas cylinder, ③ Argon gas cylinder, ④ Helium gas cylinder, ⑤ Control panel for torch, ⑥ Powder supply for the third nozzle, ⑦ Power supply for the primary anode nozzle, ⑧ Power supply for the secondary anode nozzle, ⑨ Plasma torch, ⑩ Power supply for solenoidal coil, ⑪ Solenoidal coil, ⑫ Mechanical booster pump, ⑬ Ionized vacuum gauge, ⑭ Control panel for vacuum system, ⑮ Window

Figure 1. Experimental apparatus.

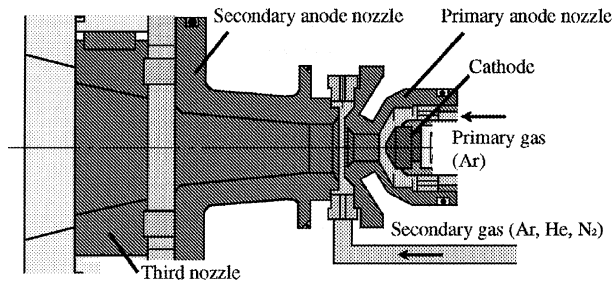

Figure 2. Plasma torch.

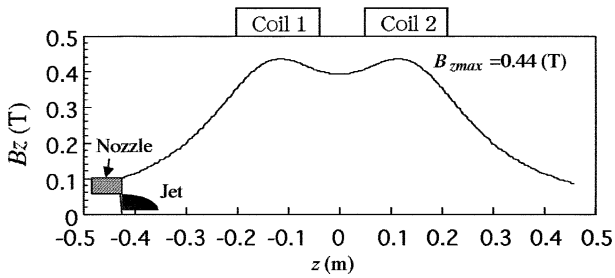

Figure 3. Axial distribution of magnetic flux density.

in the secondary anode nozzle is 6.3 kW. The total volume flow rate is 60 Sl·min^{-1} in all cases. Mixed volume flow rate of He or N_2 gas is 50 % to the total volume for each case. The plasma jet is introduced in a pipe, the diameter of which is 80 mm, keeping an operating pressure of 700 Pa, but the pressure at the inlet of the torch chamber is $5{\cdot}10^5$ Pa. The maximum magnetic flux density of 0.44 T of a mirror type can be produced by two solenoidal coils, characteristic of which is shown in *figure 3*. The main measuring location is set at the middle section of the two coils, 426 mm downstream from the nozzle exit. The experiment is conducted within the stationary conditions to make fluctuating uncertainties as small as possible.

Plasma jet is visualized by a CCD camera for an easy observation of the effects of admixing of gas and applying a magnetic field. Gas composition is measured by a quadrupole mass spectrometer by sampling the gas through the pressure tube. Gas temperature is measured by a W–Re thermocouple showing an underestimated value, since the correction is not made for radiation loss due to the difficult evaluation of the exact emissivity of the thermocouple in the steep temperature gradient with high accuracy. Gas velocity is determined by means of total and static pressure tubes. The total temperature is corrected to the static temperature corresponding to the equations (1) and (2) which are coupled through the subsonic gas velocity [9]:

$$U_g = \left\{ \frac{2\gamma}{\gamma - 1} \frac{p_s}{\rho} \left[\left(\frac{p_t}{p_s} \right)^{(\gamma-1)/\gamma} - 1 \right] \right\}^{1/2} \quad (1)$$

$$T_g = T_t - \frac{U_g^2}{2C_p} \quad (2)$$

Plasma properties, such as electron temperature and electron number density, are measured by means of a cylindrical-type Langmuir probe made of tungsten and insulated with ceramic, which is set in radial direction to suppress the effect of magnetic field. Electron density is evaluated from ion saturation current I_{is} which is not influenced so much by the applied magnetic field. The size of the probe is 0.3 mm in diameter and 3.0 mm in length. The biased voltage for the probe is swept from -20 V to $+5$ V. Plasma properties are given by the following equations [4, 10]:

$$\frac{d \ln I_p}{d V_p} = -\frac{e}{k T_e} \quad (3)$$

$$I_{is} = \kappa n_e e S_p \left(\frac{k T_e}{m_i} \right)^{1/2} \quad (4)$$

These probes can be traversed in the radial direction of the plasma jet to measure the radial distributions of those parameters in the applied magnetic field. Transport properties such as electron thermal conductivity and electron electrical conductivity [11] are given by the following equations:

$$\lambda_e = k n_e \overline{C}_e l_e \quad (5)$$

$$\sigma_e = \frac{n_e e^2}{m_e \bar{\nu}_{eH}} = e n_e \mu_e \quad (6)$$

3. EXPERIMENTAL RESULTS AND DISCUSSION

3.1. Thermofluid characteristics

Figure 4 shows the effects of the admixing of gases and of an applied magnetic field on a plasma jet. The differences of the luminescence and the jet length are shown clearly by these photos which are taken at the location between two solenoidal coils. The luminescence of an Ar/Ar (a primary gas/a secondary gas) plasma jet is the strongest compared with those of an Ar/He and Ar/N_2 plasma jets with and without magnetic field. The application of a magnetic field results also in an enhanced luminescence and an elongation of the plasma jet in all cases.

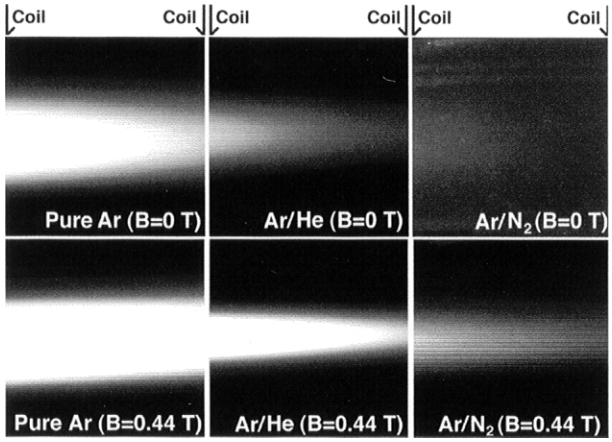

Figure 4. Effects of admixing of gases and of applying a magnetic field on a plasma jet.

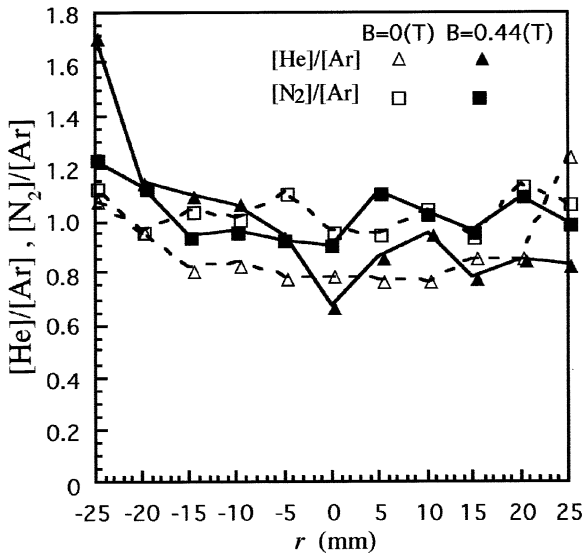

Figure 5. Radial distribution of gas concentration.

Figure 5 shows the radial distribution of the relative gas concentration ratio. The concentration ratio of He gas is decreased slightly in the core region, but is increased unsymmetrically near the wall in the applied magnetic field. On the other hand, N_2 gas concentration ratio is almost uniform in the radial direction. These results mean that He gas is not mixed uniformly with Ar gas in the radial direction compared with N_2 gas, since the complex 3-D admixing shows the unsymmetrical diffusion in the radial direction due to the large differences of density and viscosity between Ar and He even in the flowing.

Figure 6 shows the radial distribution of gas velocity. The maximum velocity in the core region amounts around 1 000 $m \cdot s^{-1}$ for an Ar/He plasma jet because

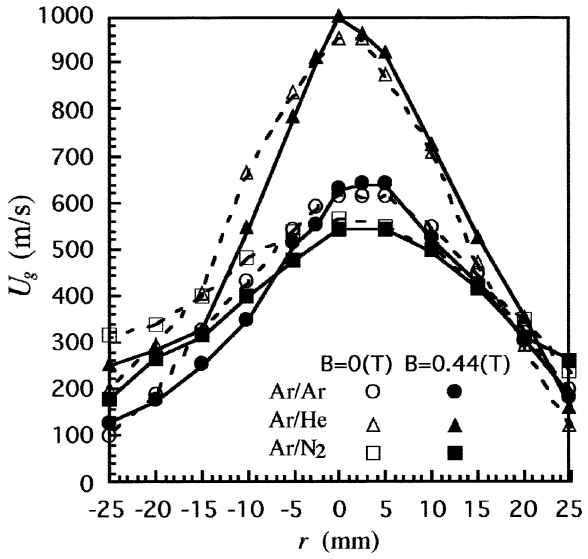

Figure 6. Radial distribution of gas velocity.

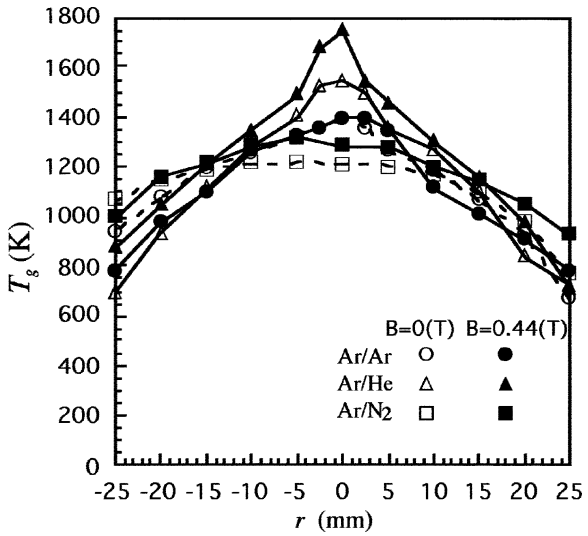

Figure 7. Radial distribution of gas temperature.

of the large net effective enthalpy per unit mass due to the small density of He. The small density results in the higher expansion, showing high Mach number effect, which results in the higher acceleration than other gases. The velocity and its radial gradient is the smallest in the case of an Ar/N_2 plasma, since the plasma jet is diffused wider in radial direction at the nozzle exit in the visualization. The wider diffusion transfers radially the larger momentum and results in the decrease in the axial momentum, that is, the decrease in the axial velocity of the jet in the downstream. Although the effect of applying a magnetic field is not so remarkable in any cases, the velocity is increased slightly in the core region and is decreased slightly near the wall.

Figure 7 shows the radial distribution of gas temperature. In all cases the maximum gas temperature values exist in the core region similar to the velocity distribution. Especially, the highest value of 1 800 K is shown in the case of an Ar/He plasma jet in an applied magnetic field. This may be caused by thermal pinch produced by the colder He gas surrounding the core region of a plasma jet and by small energy loss from little ionization. On the other hand, an Ar/N_2 plasma jet shows lower temperature in the core region compared with other cases, and the temperature gradient is moderate in the radial direction. These characteristics may result from the intensive heat transfer towards the wall due to the high thermal conductivity caused by the active dissociation and recombination and further the large radial diffusion of the jet at the nozzle exit in the visualization. Furthermore, the reason why the velocity and temperature radial profiles show the same tendency is that the heat production and heat loss in the plasma flow come from the many thermal mechanisms such as Joule heating, ionization, dissociation and recombination energies, convection, thermal conduction and radiative loss, satisfying the energy equation.

3.2. Plasma properties

Figure 8 shows the radial distribution of electron temperature. Electron temperature is considerably higher than the gas temperature as shown in *figure 7*. A ther-

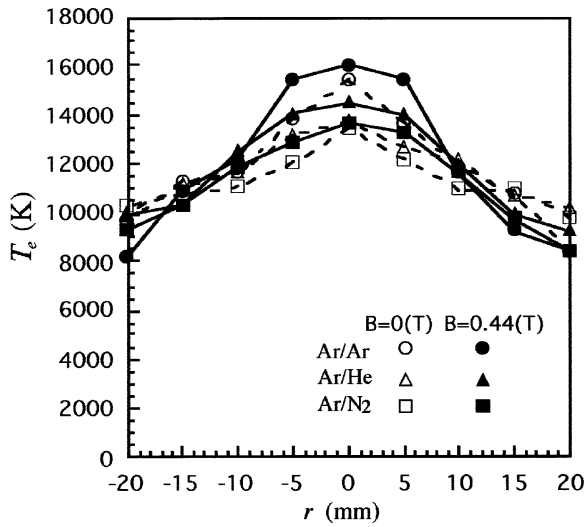

Figure 8. Radial distribution of electron temperature.

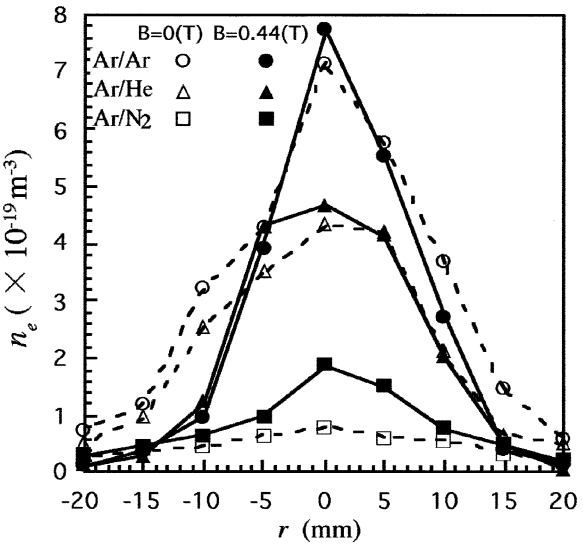

Figure 9. Radial distribution of electron number density.

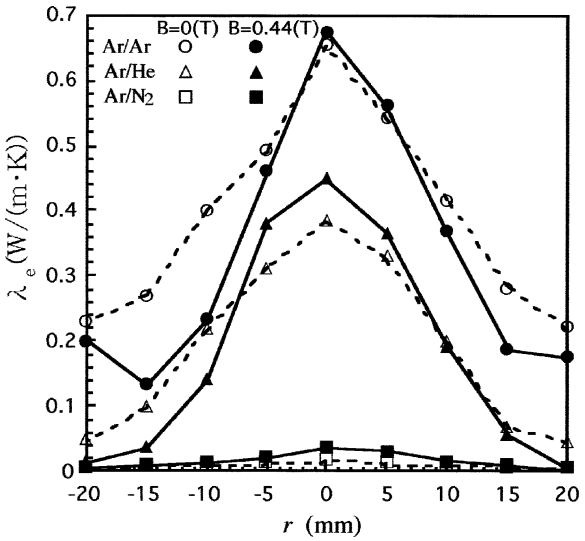

Figure 10. Radial distribution of electron thermal conductivity.

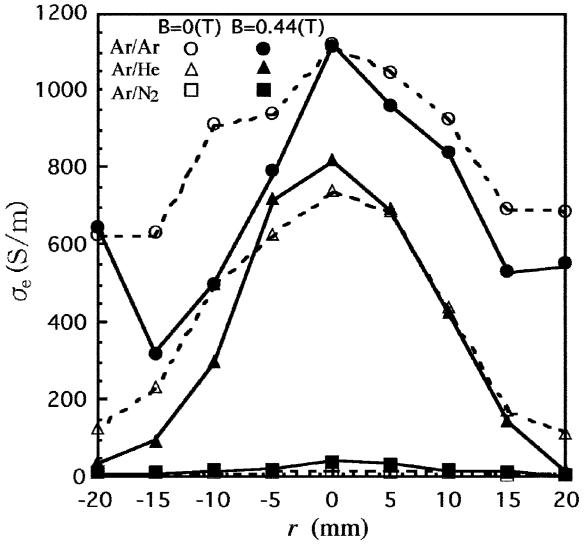

Figure 11. Radial distribution of electrical conductivity.

mal nonequilibrium is shown clearly from the result. The maximum electron temperature is shown in the case of an Ar/Ar plasma, although the maximum gas temperature is shown in the case of Ar/He. In the case of the applied magnetic field, the electron temperature is increased in the core region due to the active Joule heating production resulted from the interaction between electrical currents including the Hall current [12] and inductive electric field.

Figure 9 shows the radial distribution of electron number density. Electron number density of an Ar/Ar plasma jet in the core region is considerably larger than that of an Ar/He plasma jet, since Ar gas can be ionized easier than He gas and N_2 gas. The smallest number density is shown in an Ar/N_2 plasma jet, since most of the input power is used to dissociate N_2 gas before ionization. The electron number density is increased by applying a magnetic field in all cases. This results from the Lorentz force in the radial direction, restricting the electron diffusion in the radial direction by the magnetic lines of force, and from an increase in collision ionization between restrained electrons and heavy particles. The distribution of the number density corresponds closely to the luminous area of plasma jets as shown in *figure 4*. This implies that the electron number density correlates strongly with the radiation intensity.

3.3. Transport properties

Figure 10 shows the radial distribution of electron thermal conductivity. The effects of the gas admixing show the same tendency as the electron number density since the electron thermal conductivity is directly depending on electron number density given by equation (5). The values of Ar/Ar and Ar/He plasma jets are considerably larger than that of an Ar/N_2 plasma jet. This means that the thermal diffusion is important for the electron heat transfer of Ar/Ar and Ar/He plasma jets. On the other hand, the heat transfer of Ar/N_2 plasma jet is not governed so much by the electron thermal diffusion.

Figure 11 shows the radial distribution of electrical conductivity. The maximum of electrical conductivity appears also with an Ar/Ar plasma jet same as the

electron number density. In the case of an applied magnetic field, only the electrical conductivity in the center of an Ar/He plasma jet is increased a little and then it increases indirectly the gas temperature. However, the electrical conductivity in other regions of Ar/Ar and Ar/He plasma jets are decreased in the applied magnetic field.

4. CONCLUSION

The present study shows experimentally that the temperature and flow fields of a nonequilibrium Ar plasma jet can be influenced considerably by admixing of He or N_2 gas coupled with an applied magnetic field. The main results obtained here are summarized as follows:

(1) The concentration of He gas is relatively high near the wall, and that of N_2 gas is almost uniform across the plasma jet when He or N_2 gas is injected tangentially to produce the strong swirl flow as a secondary gas.

(2) The maximum values of gas velocity and gas temperature are found in the core region for all cases. The velocity, temperature and their gradients are also the largest in the case of an Ar/He plasma jet due to the small mass, Mach number effect and small energy loss.

(3) Electron temperature and electron number density differ depending on the kind of admixed gases. The plasma properties are the largest in the case of an Ar/Ar plasma jet and these values are further increased in the core region by applying a magnetic field because of the Lorentz force and Joule heating.

(4) The characteristics of electrical transport properties correspond nearly to that of electron number density distribution.

Acknowledgements

Completion of the experimental apparatus and the conduction of the experiment owe to the help of a technician Mr. Kazunari Katagiri at Institute of Fluid Science, Tohoku University, and also a general manager Mr. Hirobumi Sonoda and a senior researcher Mr. Naomichi Ichimura at Nippon Steel Welding Products & Engineering Co. Ltd. This research was partly supported by the Grant-in-Aid for Scientific Research from the Ministry of Education, Science, Sports and Culture, and Sumitomo Research Foundation, Japan.

REFERENCES

[1] Pfender E., Fincke J.R., Spores R., Entrainment of cold gas into thermal plasma jets, Plasma Chem. Plasma Process 11 (1991) 529–542.

[2] Fincke J.R., Chang C.H., Swank W.D., Haggard D.C., Entrainment and demixing in subsonic argon/helium thermal plasma jet, J. Thermal Spray Tech. 2 (4) (1993) 345–350.

[3] Fincke J.R., Swank W.D., Haggard D.C., Entrainment and demixing in subsonic thermal plasma jets: Comparison of measurements and predictions, Int. J. Heat Mass Tran. 37 (1994) 1673–1682.

[4] Nishiyama H., Sato T., Veefkind A., Kamiyama S., Functional enhancement of a non-equilibrium plasma jet by seeding in the applied magnetic field, Heat Mass Tran. 30 (5) (1995) 291–296.

[5] Nishiyama H., Saito T., Kamiyama S., Numerical simulation of a nonequilibrium plasma jet in an applied magnetic field using three-fluid model, Plasma Chem. Plasma Process 16 (2) (1996) 265–286.

[6] Rahmane M., Soucy G., Boulos M.I., Mass transfer in induction plasma reactors, Int. J. Heat Mass Tran. 39 (14) (1994) 2035–2046.

[7] Watanabe T., Tonoike N., Honda T., Kanzawa A., The flow, temperature and concentration fields in reactive plasmas in an inductively coupled rf discharge, J. Chem. Eng. Japan 24 (1) (1991) 25–32.

[8] Girshik S.L., Yu W., Radio-frequency induction plasmas at atomospheric pressure: mixtures of hydrogen, nitrogen, and oxygen with argon, Plasma Chem. Plasma Process 10 (1990) 515–522.

[9] Hasui A., Kitahara S., Fukushima T., Some properties of plasma jet for spraying, J. Japan Welding Soc. 36 (1967) 571–579 (in Japanese).

[10] Swift J.D., Rschwar M.J., Electrical Probes for Plasma Diagnostics, Iliffe Books, London, 1970.

[11] Mitchner M., Kruger Ch.H. Jr., Partially Ionized Gases, Wiley, New York, 1973.

[12] Sato T., Nishiyama H., Kamiyama S., Control of a non-equilibrium plasma jet by applying the magnetic field, Trans. JSME Ser. B 60 (1994) 1161–1167 (in Japanese).